Quantifying the Permafrost Heat Sink in Earth's Climate System

Jan Nitzbon[1,2], Gerhard Krinner[3], Thomas Schneider von Deimling[1,4], Martin Werner[2], Moritz Langer[1,4]

[1]Permafrost Research Section, Alfred Wegener Institute Helmholtz Centre for Polar and Marine Research, Potsdam, Germany
[2]Paleoclimate Dynamics Section, Alfred Wegener Institute Helmholtz Centre for Polar and Marine Research, Bremerhaven, Germany
[3]Institut des Géosciences de l'Environnement, CNRS/Université Grenoble Alpes, Grenoble, France
[4]Geography Department, Humboldt-Universität zu Berlin, Berlin, Germany

Key Points:

- We provide the first estimate of heat uptake through both warming and thawing of Arctic terrestrial permafrost.
- From 1980 to 2018, $3.9^{+1.5}_{-1.7}$ ZJ of heat have been taken up in the permafrost region, about 45 % of which through melting of ground ice.
- Thawing of permafrost is a heat sink similar in magnitude to other components of Earth's cryosphere.

Corresponding author: Jan Nitzbon, jan.nitzbon@awi.de

Abstract

Due to an imbalance of incoming and outgoing radiation at the top of the atmosphere, excess heat has been accumulating in Earth's climate system in recent decades, driving global warming and climatic changes. To date it has not been quantified how much of this excess heat is being used for the melting of ground ice in the terrestrial permafrost region. Here, we diagnose changes in sensible and latent heat contents in the northern terrestrial permafrost region from ensemble simulations of a numerical permafrost model. We find that about $3.9^{+1.5}_{-1.7}$ ZJ of heat, of which $1.7^{+1.4}_{-1.5}$ ZJ (45 %) were used to melt ground ice, were taken up by permafrost from 1980 to 2018. This suggests that permafrost is a persistent heat sink similar in magnitude to other components of the cryosphere that requires an explicit consideration in assessments of the Earth's energy imbalance.

Plain Language Summary

During the past decades planet Earth has received more energy from the sun than it emitted back into space. This led to a surplus of energy which is causing global warming and climate change. While the majority of this surplus energy is being absorbed by Earth's oceans, some part of it is used for the melting of ice contained in permafrost ground. However, we do not know how much. In this study, we use a computer model to calculate how much energy has been taken up by permafrost in the Arctic during the past four decades. We find that about 3.9 sextillion Joules of energy were taken up by permafrost from 1980 to 2018. About 45 % of this energy has been used to melt ice contained in the ground, while the remaining energy caused warming of the ground. Our findings suggest that a similar amount of energy is taken up by permafrost as it is absorbed by other large ice bodies on Earth, such as ice sheets, glaciers, or sea ice. Our study implies that the energy taken up by permafrost needs to be considered in global assessments of Earth's energy budget which has not been the case so far.

1 Introduction

Due to the positive difference between incoming and outgoing radiation at the top of its atmosphere, the Earth has been accumulating heat over the past decades, which is referred to as Earth's Energy Imbalance (EEI) (Hansen et al., 2005; von Schuckmann et al., 2016). The EEI is a more robust measure of global warming and climate change than global mean surface temperatures, because it is less prone to annual-to-decadal fluctuations associated with natural climate variability (von Schuckmann et al., 2016, 2020). The great majority (about 90 %) of the excess heat is taken up by Earth's oceans (Church et al., 2011; von Schuckmann et al., 2020; Frederikse et al., 2020), causing their thermal expansion which is the main contributor to global sea level rise (Group, 2018; Edwards et al., 2021). Only a small fraction (1-2 %) of excess heat ends up in the atmosphere. This is reflected in an increase in global mean surface temperatures and humidity (Stoy et al., 2022). Similar shares of the remaining heat cause warming of Earth's continental landmasses (5-6 %), and melting of its ice masses (3-4 %), addressed in more detail by T. Slater et al. (2021).

However, observation-based estimates of the heat taken up by the cryosphere (e.g., (Church et al., 2011; von Schuckmann et al., 2020; T. Slater et al., 2021)), do not accurately take into account the northern terrestrial permafrost region, which is the largest non-seasonal component of Earth's cryosphere in terms of spatial extent. In the permafrost region, net positive ground heat fluxes cause both warming of the subsurface (change in sensible heat content), and melting of ground ice (change in latent heat content). While sparsely-distributed temperature records from boreholes allow rough estimates of the overall sensible heat uptake in the permafrost region (Biskaborn et al., 2019; Cuesta-Valero, García-García, Beltrami, González-Rouco, & García-Bustamante, 2021), we are not aware of comparable long-term records of changes in ground water/ice contents that would al-

low to estimate the overall latent heat uptake in a similar manner. Permafrost thaw and ground ice melt are being reported to occur across the Arctic (Jorgenson et al., 2006; Liljedahl et al., 2016; Farquharson et al., 2019), and projected to continue in the coming decades and centuries (Lawrence et al., 2012; Burke et al., 2020). Hence, a potentially substantial heat sink, namely the latent heat uptake through melting of ground ice in the permafrost region, has to date not been quantified and is therefore missing in global assessments of Earth's energy budget (von Schuckmann et al., 2020; Forster et al., 2021).

Apart from long-term observations, numerical models provide an alternative possibility to constrain plausible ranges for heat contents in and fluxes between different compartments of the climate system. For example, Cuesta-Valero, García-García, Beltrami, and Finnis (2021) have diagnosed Earth's heat inventory from Earth system models (ESMs) participating in the Climate Model Intercomparison Project Phase 5 (CMIP5). However, the land surface models (LSMs) used in CMIP5 have several shortcomings which disqualify their simulations from being used to diagnose permafrost heat uptake. First, several of the models do not represent freezing and thawing of ground water, and hence they do not partition ground heat into sensible and latent. Second, several studies pointed out that the subsurface domain of the models is too shallow to accurately represent long-term ground heat storage (Cuesta-Valero et al., 2016; Hermoso de Mendoza et al., 2020; Steinert, González-Rouco, Melo Aguilar, et al., 2021). Third, the LSMs lack a realistic prescription of ground ice contents, and in particular do not represent excess ice which is abundant in lowlands of the continuous permafrost zone (Olefeldt et al., 2016). Therefore, more tailored models are required to realistically assess the contribution of permafrost heat uptake to Earth's energy budget.

Here, we use the permafrost model CryoGridLite (Langer, Nitzbon, Groenke, et al., 2022) to simulate changes in sensible and latent heat contents within the northern terrestrial permafrost region. We diagnose the simulations to provide a first, conservative estimate of the heat uptake through both warming and thawing of permafrost during the past four decades (1979-2018). We further investigate spatial patterns of heat uptake in the study region, and put our findings into context with previous assessments of EEI, and in particular with the heat uptake through other components of Earth's cryosphere.

2 Methods

2.1 Model Setup

We conducted ensemble simulations with the transient one-dimensional permafrost model CryoGridLite (Langer, Nitzbon, Groenke, et al., 2022) which is simplified fast version of CryoGrid3 (Westermann et al., 2016). We closely followed Langer, Nitzbon, Groenke, et al. (2022) to conduct distributed model simulations for the northern terrestrial permafrost region on a 1°-latitude by 1°-longitude grid. Below, we provide a short description of the model setup and the simulations. For details on the representation and implementation of physical processes, the parameterization, as well as a comprehensive evaluation of the simulated transient thermal regimes of CryoGridLite, we refer to Langer, Nitzbon, Groenke, et al. (2022).

CryoGridLite solves the one-dimensional heat equation under consideration of phase change of soil water using an implicit backward integration scheme for enthalpy H [$\mathrm{J\,m^{-3}}$] as the state variable:

$$\frac{\partial H}{\partial t} = \frac{\partial}{\partial z}\left(k\frac{\partial\, T(H)}{\partial z}\right)\,, \tag{1}$$

where k [$\mathrm{W\,m^{-2}\,K^{-1}}$] is the thermal conductivity, T [K] the subsurface temperature, and the coordinate z corresponds to the depth below the ground surface. The enthalpy (H)

is composed of sensible (H_S) and latent (H_L) heat contents of the ground:

$$H(T, \theta_w) = H_S + H_L = C\,T + L_{sl}\,\theta_w\ , \tag{2}$$

where C [$J\,m^{-3}\,K^{-1}$] is the volumetric heat capacity, L_{sl} [$J\,m^{-3}$] the volumetric latent heat of fusion of water, and θ_w [-] the volumetric liquid water content.

The heat equation (1) is solved on a discrete subsurface grid consisting of 278 cells with increasing thickness extending down to a depth of 550 m. The deep model domain allows a much more realistic representation of the long-term transient thermal regime and heat reservoirs than the shallow subsurface representation typical for LSMs (Hermoso de Mendoza et al., 2020; Steinert, González-Rouco, Vrese, et al., 2021). At the bottom of the model domain, a geothermal heat flux according to Davies (2013) was prescribed as boundary condition. At the surface, the model was forced by timeseries of daily mean air temperatures and snowfall rates. These meteorological forcing data were based on ERA-Interim reanalysis data (Dee et al., 2011) spanning the period from 1980 to 2018 which is also the main analysis period of our study. To account for the modification of the heat exchange between the ground and the atmosphere through snow, CryoGridLite comprises a snow scheme which simulates the dynamic build-up and melting of a seasonal snowpack.

The ground stratigraphies which determine the thermal properties of the subsurface were based on the Open-ECOCLIMAP global database of land surface parameters (Masson et al., 2003; Faroux et al., 2013), the soil organic carbon map for the permafrost region by (Hugelius et al., 2014), and the global map of soil thicknesses by (Pelletier et al., 2016). CryoGridLite does not comprise a dynamic hydrology scheme such that the volumetric composition in terms of mineral, organic, and water/ice contents remains constant throughout the simulation. However, the uncertainty and variability with respect to the subsurface hydrological conditions and their effect on the heat transfer have been addressed by performing ensemble simulations with different water/ice contents and distributions (see Section 2.2).

We performed a model spin-up to establish a transient equilibrium state of the ground thermal regime at the beginning of the analysis period. For this, we applied anomalies derived from paleo-climate simulations by the Mk3L climate model of the Commonwealth Scientific and Industrial Research Organisation (CSIRO) (Phipps et al., 2013) to the ERA-Interim data. The spin-up consisted of two phases: First, a single simulation with default parameter values was run from year 500 to 1600 for each grid cell of the pan-Arctic model domain. Second, an ensemble of 50 simulations with variations in the model parameters was run from 1600 to 1980. Our results are based on the multi-parameter ensemble for the subsequent period from 1980 until 2018 for which no anomalies have been applied to the ERA-Interim forcing data.

2.2 Ensemble Simulations

The heat uptake of the ground and its partitioning in the permafrost region are affected by various environmental factors. While the ground thermal regime and, thus, the sensible heat content are crucially affected by the seasonal snow cover (A. G. Slater et al., 2017; Jan & Painter, 2020; Zweigel et al., 2021, e.g.), potential changes in the latent heat content are primarily affected by the amount and the distribution of ground ice. To account for both the uncertainty and the spatial variability associated with these environmental factors, we conducted an ensemble of 50 independent simulations with a random variation of several parameters for each grid cell of the model domain. Following Langer, Nitzbon, Groenke, et al. (2022), we varied the model parameters prescribing the depths and pore water/ice contents of several subsurface layers, as well as the threshold for the maximum height of the snow pack.

In addition to the variation of pore ice/water, we also considered the presence of excess ice, based on the map by Brown et al. (1997). Specifically, we increased the ice content by a volumetric fraction (χ) in a range from the surface ($z = 0$) down to a depth z_χ and reduced the sediment fraction in this part of the stratigraphy by a factor $1-\chi$. The depth (z_χ) and the amount (χ) of excess ice have been varied in the parameter ensemble using uniform prior probabilities based on the ground ice map ($z_\chi \in [10\,\mathrm{m}, 20\,\mathrm{m}]$; $\chi_{\mathrm{L/M/H}} \in [0.0, 0.1]/[0.1, 0.2]/[0.2, 0.3]$ for low/medium/high ground ice content).

With these ensemble simulations we captured a wide range of environmental conditions which determine the ground thermal regime on a local scale. At the same time, the ensemble simulations allowed us to estimate confidence intervals for the model diagnostics.

3 Results and Discussion

3.1 Net Heat Uptake by the Northern Terrestrial Permafrost Region

According to our simulations, $3.9^{+1.5}_{-1.7}\,\mathrm{ZJ}$ ($1\,\mathrm{ZJ} = 10^{21}\,\mathrm{J}$; ranges correspond to 90th and 10th percentiles) of heat accumulated in the landmass of the northern terrestrial permafrost region during the almost four decades from 1980 to 2018 (Table 1, ERA-Interim). This number increases to $5.1^{+1.8}_{-2.0}\,\mathrm{ZJ}$ when the final two decades of the spin-up period (1960-1979) are included, allowing for a direct comparison to the estimates by von Schuckmann et al. (2020) (Table 1, vS20). The share of permafrost heat uptake in the EEI of about 358 ZJ (1971-2018) reported by von Schuckmann et al. (2020) would be about 1.3 %, comparable to the share of the atmosphere. The importance of permafrost relative to the continental and the cryospheric heat uptake, respectively, is even more substantial (Figure 1 a,b).

Table 1. Heat accumulation and ground ice melt for different periods in comparison to estimates by von Schuckmann et al. (2020) (vS20) and T. Slater et al. (2021) (Sl21). Confidence intervals correspond to the 95th and 5th percentile, respectively.

Diagnostic	Symbol	Unit	1980-2018 (ERA-Interim)	1960-2018 (vS20)	1994-2017 (Sl21)
Total heat change	ΔH	ZJ	$3.9^{+1.5}_{-1.7}$	$5.1^{+1.8}_{-2.0}$	$2.7^{+1.0}_{-1.0}$
Sensible heat change	ΔH_S	ZJ	$2.2^{+0.7}_{-0.7}$	$2.8^{+0.9}_{-0.9}$	$1.6^{+0.5}_{-0.5}$
Share in global land heat change[a]	-	%	11.3	11.8	12.6
Latent heat change	ΔH_L	ZJ	$1.7^{+1.4}_{-1.5}$	$2.2^{+1.7}_{-1.9}$	$1.1^{+0.9}_{-0.9}$
Share in global cryosphere heat change[b]	-	%	11.0	13.1	9.2
Permafrost ground ice melt rate	m_pi	Gt yr^{-1}	137.6	115.5	143.9
Share in global ice imbalance[c]	-	%	-	-	10.7

[a] calculated as $\Delta H_\mathrm{S}/\Delta\mathrm{GHC}$ where ΔGHC is the change in global ground heat content estimated by (von Schuckmann et al., 2020) which comprises the permafrost region.

[b] calculated as $\Delta H_\mathrm{L}/(\Delta\mathrm{CHC} + \Delta H_\mathrm{L})$ where ΔCHC is the change in heat content of cryosphere components estimated by von Schuckmann et al. (2020) which disregards permafrost and snow. Note that the estimate of ΔCHC is only available until 2017, such that the period 1960-2017 was taken to calculate the share.

[c] calculated as $m_\mathrm{pi}/(m_\mathrm{fi} + m_\mathrm{gi} + m_\mathrm{pi})$ where m_fi and m_gi are estimates for mean melt rates of floating and grounded ice during the same period, provided by T. Slater et al. (2021).

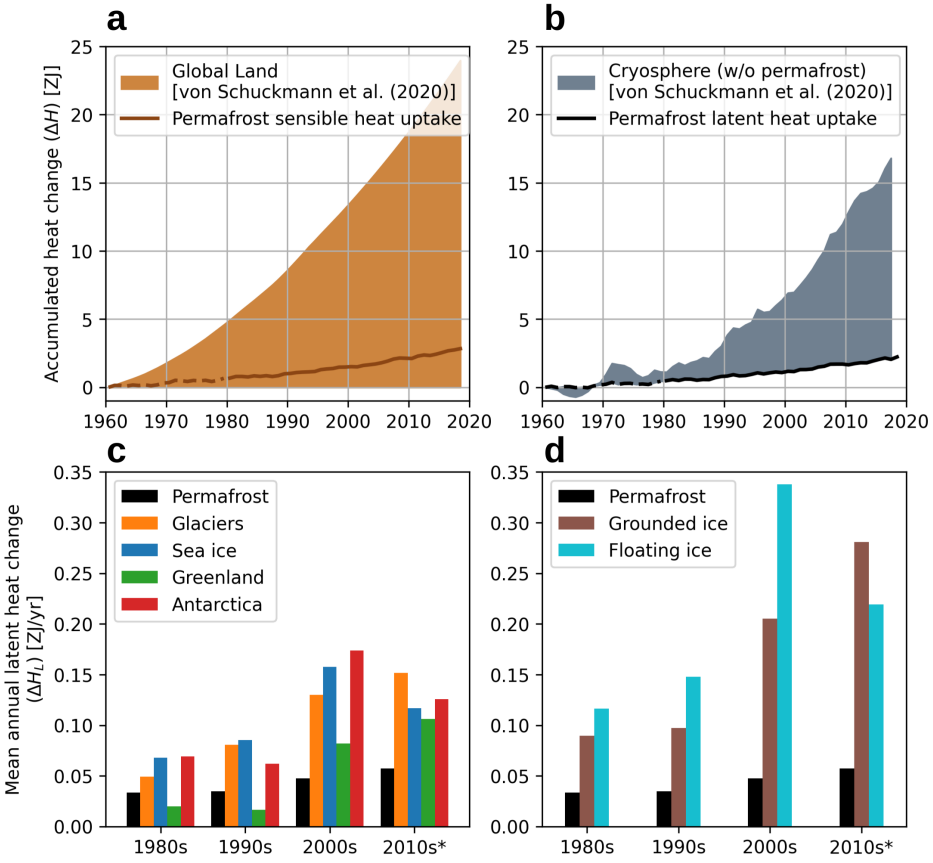

Figure 1. a,b: Simulated accumulation of sensible (a) and latent (b) heat in the northern terrestrial permafrost region from 1960 to 2018. For comparison, the filled areas indicate the heat accumulation in the global continental landmass (a) and the cryosphere (without permafrost, b) according to von Schuckmann et al. (2020). c,d: Comparison of mean annual heat changes during the past four decades for different components of the cryosphere (c), and for different types of ice (d). Data for permafrost are from this study and data for the remaining cryosphere from von Schuckmann et al. (2020) and Straneo et al. (2020). *only from 2010 to 2017.

We diagnosed that $2.2^{+0.7}_{-0.7}$ ZJ (1980-2018; 55 % of the total heat uptake) of sensible heat have accumulated in the permafrost region's landmass which is equivalent to about 11.3 % of the global land heat uptake in that period estimated by Cuesta-Valero, García-García, Beltrami, González-Rouco, and García-Bustamante (2021) and reported in von Schuckmann et al. (2020) (Figure 1 a). Note that this proportion is very similar to the proportion of the land area contained in the model domain to the global land area (12.3 %).

A similar amount of heat taken up in the permafrost region is used for the melting of ground ice. We diagnosed that $1.7^{+1.4}_{-1.5}$ ZJ (1980-2018; 45 % of the total heat uptake) of latent heat were taken up by the subsurface of the model domain through melting of ground ice. This corresponds to about 11.0 % of the heat accumulation in Earth's cryosphere, if the contribution of permafrost would be added to the estimate by von Schuckmann et al. (2020) for the cryosphere without permafrost (Figure 1 b). Converting the latent heat change in permafrost into a mean annual ground ice melt rate (using $L_{\mathrm{sl}} = 330000\,\mathrm{J\,kg^{-1}}$) results in a value of $m_{\mathrm{pi}} = 143.9\,\mathrm{Gt\,yr^{-1}}$ (1994-2017) which is about 10.7 %

of the combined melt rates of grounded ice ($543\,\mathrm{Gt\,yr^{-1}}$) and floating ice ($653\,\mathrm{Gt\,yr^{-1}}$) estimated for the same period (T. Slater et al., 2021) (Table 1, Sl21).

Our findings point out a duality of permafrost ground: on the one hand it is a component of Earth's continental landmass, on the other hand a component of its cryosphere. As part of the landmass, the permafrost region is warming at a similar rate as the landmasses outside the permafrost region. As part of the cryosphere, permafrost constitutes a heat sink which is substantial compared to the remaining cryosphere during the past decades, especially when compared to the different components of the cryosphere.

3.2 Comparison to Other Components of the Cryosphere

While the latent heat uptake by permafrost is steadily increasing from about $0.03\,\mathrm{ZJ\,yr^{-1}}$ in the 1980s to about $0.06\,\mathrm{ZJ\,yr^{-1}}$ in the 2010s (Figure 1 c), the other components show an even more pronounced increase during this period, which is particularly strong for Greenland and Antarctica from the 1990s to the 2000s. Consequently, the relative share of permafrost in the heat uptake by the entire cryosphere declined from about 16 % during the 1980s (1980-1989) to about 11 % during the 2010s (2010-2017), suggesting a decreasing importance of the permafrost heat sink relative to the other cryospheric heat sinks. We hypothesize that this is due to a slower response of ground ice (permafrost) to recent warming compared to that of floating ice (ice shelves, sea ice) and grounded ice (ice sheets, glaciers) (Figure 1 d), which are directly exposed to the atmosphere. Permafrost in turn is primarily an subsurface phenomenon protected from the atmosphere through the active layer as well as isolating buffer layers such as vegetation (Shur & Jorgenson, 2007; Stuenzi et al., 2021), which can delay the response to warming at the surface. The considered period of about four decades is, however, too short to draw firm conclusions regarding the longer-term strength of the different cryospheric heat sinks. This is also indicated by the fact that while the heat uptake through sea ice, Greenland, and Antarctica show a marked inter-decadal variability, the permafrost heat sink is more persistent and shows a steady positive trend with little inter-decadal variability.

All cryospheric components including permafrost ground ice have in common that their capacity as a heat sink is limited by the amount of ice stored in them. These sinks for latent heat are thus qualitatively different from the sinks for sensible heat provided by the ocean, the land, and the atmosphere. With the projected shrinking of Earth's grounded, floating and ground ice bodies (Fox-Kemper et al., 2021), the cryospheric heat sinks will also eventually shrink, implying that a larger fraction of heat has to be stored in the oceans, land, and the atmosphere. Indeed, a decrease of the cryospheric heat storage and a concurrent increase in the shares of the ocean and atmosphere during the past decade has been reported (von Schuckmann et al., 2020). This shift in the partitioning of the EEI happens along with a current trend towards larger absolute values of the EEI (Loeb et al., 2021).

3.3 Contrasting Patterns of Sensible and Latent Ground Heat Changes

Except for very few locations, the entire northern permafrost region has been simulated to constitute a net heat sink during the analysis period (1980-2018; Figure 2 c), indicating that permafrost ground has been warming or thawing (or both) across the Arctic during the last decades. Our simulations further suggest contrasting spatial patterns of sensible versus latent heat uptake. The sensible heat change is most pronounced in areas featuring cold permafrost, i.e., the northernmost latitudes as well as a vast portion of central eastern Siberia (Figure 2 a), roughly coinciding with the zone of continuous permafrost. The latent heat change in turn is dominating in the southern part of the model domain, i.e., in a band from central and southern Alaska through Canada and the southern coast of the Hudson Bay to northern Quebec, as well as from northern Finnoscandia through western and southern Siberia, terminating at the Sea of Okhotsk, coincid-

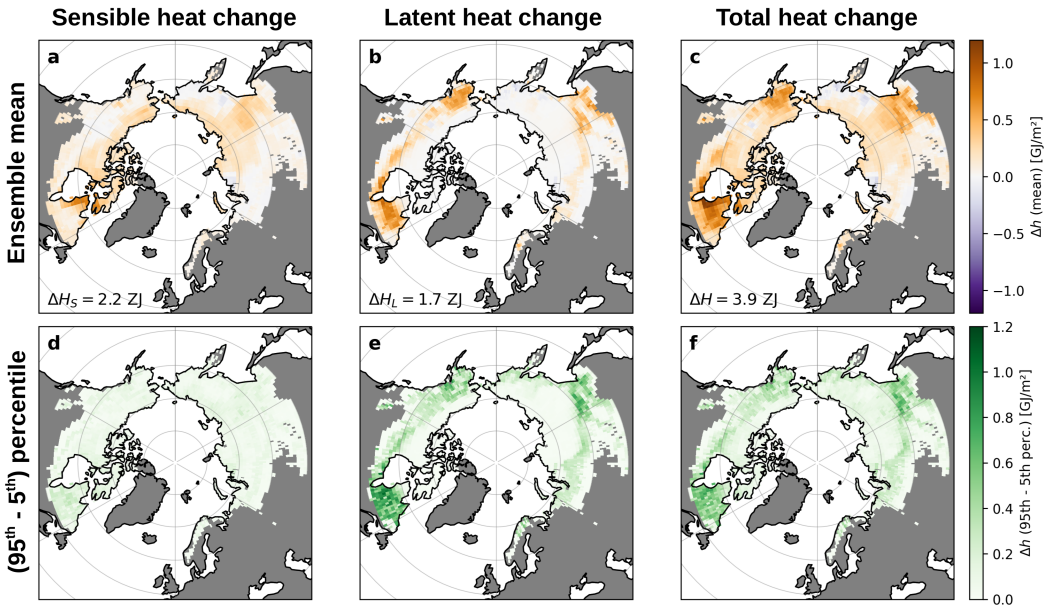

Figure 2. For each 1°-by-1° grid cell of the model domain, the maps are showing the ensemble mean (a,b,c) and the difference between the 95th and 5th percentiles (d,e,f) of the simulated changes in sensible (a,d), latent (b,e), and total (c,f) ground heat contents from 1980 to 2018.

ing with the transitional region between the discontinuous and the continuous permafrost zones (Figure 2 b).

We identified three sub-regions of the model domain for which particularly high rates of (mainly latent) heat uptake have been simulated: (i) the land area south and east of Hudson Bay in eastern Canada, (ii) the southern part of Alaska (south of the Brooks range), and (iii) the region in southeast Siberia west of the Sea of Okhotsk. For the region surrounding the Hudson Bay, we hypothesize that the marked changes in permafrost heat content have been driven by a strong increase in air temperatures and a concurrent shift in the sea ice season which potentially affects the amount and timing of snowfall (Mudryk et al., 2018). Similar mechanisms might cause patterns of climatic variability that can explain also the marked changes in the other two regions (ii,iii) which are as well adjacent to the southern margin of the seasonally sea-ice covered ocean. Notably, the simulated sensible heat changes are more homogeneously distributed, with only the region directly northeast to the Hudson Bay showing exceptionally high ground warming (Figure 2 a).

To better understand the co-variation of changes in sensible and latent heat contents, Figure 3 shows scatter plots of the respective linear trends for all grid cells of the pan-Arctic model domain. For the great majority (85.0 %) of the grid cells, both latent and sensible heat contents are showing positive trends during the simulation period. The sensible heat trends show a bimodal distribution with one mode being slightly positive, and the second mode being substantially positive at about $5\,\mathrm{MJ\,m^{-2}\,yr^{-1}}$. The latent heat trends in turn follow a unimodal distribution which has its mode at slightly positive values, but which has a long tail towards more positive values of up to about $20\,\mathrm{MJ\,m^{-2}\,yr^{-1}}$. In other words, while for the majority of locations the ground is warming but not thawing, there is also a substantial amount of locations, where permafrost is thawing but which show little warming. The coloring of the scatter points in Figures 3 a and b further reveals that the locations with substantial warming are characterized by cold mean annual

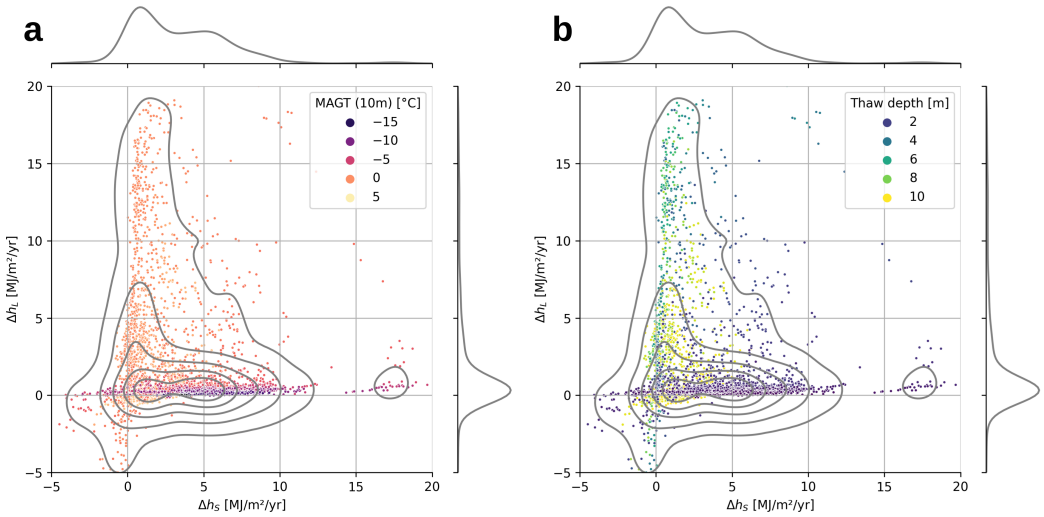

Figure 3. Scatter plots of the trends of ensemble-mean latent (Δh_{L}) versus sensible (Δh_{S}) heat contents for each grid cell of the model domain (1980 to 2018). Marker colors indicate the mean annual ground temperature (MAGT) at 10m depth (a), and the maximum thaw depth (b), respectively. Gray lines indicate kernel density estimates of the joint and marginal distributions of the trends.

ground temperatures (MAGT $< -5\,^{\circ}\mathrm{C}$) and shallow maximum thaw depths (TD $< 2\,\mathrm{m}$). At the same time, those locations which show substantial thawing are characterized by MAGT close to $0\,^{\circ}\mathrm{C}$, and a wide range of thaw depths mostly exceeding 2 m. Otherwise, numerous locations are showing small changes in heat content and at the same time large thaw depths. These correspond to permafrost-free areas which have undergone full permafrost degradation already in the past. Overall, considering changes and trends in sensible and latent ground heat contents complements the traditional approach of assessing the thermal state of permafrost in terms of ground temperatures and thaw depths (Biskaborn et al., 2019; S. L. Smith et al., 2022).

3.4 Limitations and Implications

An observation-based assessment of the heat uptake through terrestrial permafrost is not only limited by the sparsity of long-term monitoring sites across the permafrost region, but necessarily incomplete since changes in latent heat contents are not being monitored systematically. On the one hand this concerns the melting of pore ice, which could be measured as changes in the liquid water content in the active and permafrost layers (Nicolsky & Romanovsky, 2018). On the other hand, the melting of excess ice manifesting in subsidence of the ground surface would requires monitoring as well, which is, however, still technically challenging (Liu & Larson, 2018).

Our model-based assessment compensates this lack of observations by providing consistent estimates of both sensible and latent heat changes across the northern terrestrial permafrost region. Nevertheless, it should be considered a first-order approximation, as it is subject to several sources of uncertainty and some real-world complexities are missing in our model. For instance, there is very limited knowledge on the pan-Artic distribution of ground ice at present, which constitutes the primary source of uncertainty for our model-based estimate of latent heat uptake. We addressed this factor of uncertainty by randomly varying the ground ice contents and distribution in our ensemble sim-

ulations. Consequently, the range between the 5th and 95th percentiles of estimated pan-Arctic latent heat uptake (2.9 ZJ) is about two-fold of the corresponding range for the sensible heat uptake (1.4 ZJ) (Table 1, ERA-Interim). Unlike for other components of the cryosphere, the permafrost ground ice contents cannot be observed directly, for example through remote sensing. Hence, estimates of ground ice distribution still rely on coarse mapping (Brown et al., 1997; O'Neill et al., 2019; Strauss et al., 2021) or modeling (Lacelle et al., 2022) approaches, but a recent pan-Arctic ground ice product is not available. Further shortcomings of our model are the lack of a surface energy balance calculation, static subsurface water contents, no dedicated treatment of vegetation, and a simplified snow scheme. Despite these shortcomings, it captures the essential physical mechanisms to assess the transport and storage of heat within the subsurface and its partitioning during the phase change of ground water, and is capable of reproducing recent borehole temperature evolution well (Langer, Nitzbon, Groenke, et al., 2022).

Overall, we consider our model-based estimate of the permafrost heat sink to be valid but probably conservative for the following reasons: First, we did not take into account thaw processes acting in ice-rich permafrost terrain, so-called thermokarst. These processes – also referred to as abrupt thaw – are increasingly abundant in a warming Arctic and involve the thawing of permafrost containing excess ice as well as the melting of massive ground ice bodies (Turetsky et al., 2019, 2020). Thermokarst activity thus involves a considerable uptake of latent heat, and has been documented to occur also in areas featuring cold permafrost (Farquharson et al., 2019; Nitzbon et al., 2020) which otherwise are primarily a sink for sensible heat. While there are recent advances in modeling thermokarst (Lee et al., 2014; Westermann et al., 2016; Aas et al., 2019), global assessments are still limited by the lack of information on the distribution of ground ice.Second, our model domain only comprises the northern terrestrial permafrost region, such that we did not consider warming and thawing of permafrost on the Tibetean plateau, in Alpine regions, and in Antarctica. The heat uptake through thawing of submarine permafrost was also not assessed in our analysis. While the net heat change in these permafrost-underlain areas is very likely outweighed by the northern terrestrial permafrost region, they are likely to also constitute a net heat sink in recent decades (S. L. Smith et al., 2022; Wilkenskjeld et al., 2022).

Despite these limitations, our findings underline the importance of the northern permafrost region as a component of the terrestrial cryosphere which is of relevance to the functioning of the global climate system beyond its dormant carbon pool. Hence, it demands improved representation in LSMs and ESMs. Key steps to achieve this include, for example, (i) increasing the depth of the subsurface (Steinert, González-Rouco, Vrese, et al., 2021; González-Rouco et al., 2021), (ii) representing excess ice melt and thermokarst (Lee et al., 2014), and (iii) parameterizing subgrid-scale heterogeneity and lateral fluxes (Aas et al., 2019; N. D. Smith et al., 2022).

4 Conclusions

We have provided a first estimate of heat uptake through Arctic terrestrial permafrost in recent decades. We conclude that northern permafrost constitutes a significant heat sink in Earth's climate system, which is peculiar due to its duality as a part of the continental landmass and a component of the cryosphere. Approximately similar amounts of sensible and latent heat have been taken up in the northern permafrost region during the past four decades, causing both warming and thawing of permafrost ground. While previous assessments of EEI have only considered the warming of the continental landmass, our first estimate of the contribution of permafrost thaw suggests that melting of ground ice is comparable in magnitude to the melting of ice in other major components of the cryosphere. It should thus explicitly be taken into account in future assessments of Earth's energy and ice imbalances. To achieve this, it is necessary to complement current long-term monitoring efforts of permafrost as an essential climate variable through

distributed measurements of (i) depth-resolved ground water/ice contents, and (ii) ground subsidence due to excess ice melt. For improved model-based assessments of the permafrost heat sink, a most valuable input would be a revised map of the contents, types, and distribution of ground ice encompassing the entire terrestrial Arctic.

Acknowledgments

The CryoGridLite model code is available from `https://zenodo.org/record/6619537` (Langer, Nitzbon, & Oehme, 2022a). The input data required for pan-Arctic simulations are available from `https://zenodo.org/record/6619212` (Langer, Nitzbon, & Oehme, 2022b). Model output used for the results presented in this article is available from `https://zenodo.org/record/6619260` (Langer, Nitzbon, & Oehme, 2022c).

This work was supported by a grant of the German Federal Ministry of Education and Research (BMBF, project PermaRisk, grant no. 01LN1709A).

J. Nitzbon acknowledges funding through the AWI INSPIRES program.

References

Aas, K. S., Martin, L., Nitzbon, J., Langer, M., Boike, J., Lee, H., ... Westermann, S. (2019). Thaw processes in ice-rich permafrost landscapes represented with laterally coupled tiles in a land surface model. *The Cryosphere*, *13*(2), 591–609. doi: 10.5194/tc-13-591-2019

Biskaborn, B. K., Smith, S. L., Noetzli, J., Matthes, H., Vieira, G., Streletskiy, D. A., ... Lantuit, H. (2019). Permafrost is warming at a global scale. *Nature Communications*, *10*, 264. doi: 10.1038/s41467-018-08240-4

Brown, J., Ferrians Jr., O. J., Heginbottom, J. A., & Melnikov, E. S. (1997). *Circum-Arctic map of permafrost and ground-ice conditions.* U.S. Geological Survey. doi: 10.3133/cp45

Burke, E. J., Zhang, Y., & Krinner, G. (2020, September). Evaluating permafrost physics in the Coupled Model Intercomparison Project 6 (CMIP6) models and their sensitivity to climate change. *The Cryosphere*, *14*(9), 3155–3174. doi: https://doi.org/10.5194/tc-14-3155-2020

Church, J. A., White, N. J., Konikow, L. F., Domingues, C. M., Cogley, J. G., Rignot, E., ... Velicogna, I. (2011). Revisiting the Earth's sea-level and energy budgets from 1961 to 2008. *Geophysical Research Letters*, *38*(18). doi: https://doi.org/10.1029/2011GL048794

Cuesta-Valero, F. J., García-García, A., Beltrami, H., & Finnis, J. (2021). First assessment of the earth heat inventory within CMIP5 historical simulations. *Earth System Dynamics*, *12*(2), 581–600. doi: 10.5194/esd-12-581-2021

Cuesta-Valero, F. J., García-García, A., Beltrami, H., González-Rouco, J. F., & García-Bustamante, E. (2021). Long-term global ground heat flux and continental heat storage from geothermal data. *Climate of the Past*, *17*(1), 451–468. doi: 10.5194/cp-17-451-2021

Cuesta-Valero, F. J., García-García, A., Beltrami, H., & Smerdon, J. E. (2016). First assessment of continental energy storage in CMIP5 simulations. *Geophysical Research Letters*, *43*(10), 5326–5335. doi: https://doi.org/10.1002/2016GL068496

Davies, J. H. (2013). Global map of solid Earth surface heat flow. *Geochemistry, Geophysics, Geosystems*, *14*(10), 4608–4622. doi: 10.1002/ggge.20271

Dee, D. P., Uppala, S. M., Simmons, A. J., Berrisford, P., Poli, P., Kobayashi, S., ... Vitart, F. (2011). The ERA-Interim reanalysis: configuration and performance of the data assimilation system. *Quarterly Journal of the Royal Meteorological Society*, *137*(656), 553–597. doi: 10.1002/qj.828

Edwards, T. L., Nowicki, S., Marzeion, B., Hock, R., Goelzer, H., Seroussi, H., ...

Zwinger, T. (2021). Projected land ice contributions to twenty-first-century sea level rise. *Nature*, *593*(7857), 74–82. doi: 10.1038/s41586-021-03302-y

Faroux, S., Kaptué Tchuenté, A. T., Roujean, J.-L., Masson, V., Martin, E., & Le Moigne, P. (2013). ECOCLIMAP-II/Europe: a twofold database of ecosystems and surface parameters at 1 km resolution based on satellite information for use in land surface, meteorological and climate models. *Geoscientific Model Development*, *6*(2), 563–582. doi: 10.5194/gmd-6-563-2013

Farquharson, L. M., Romanovsky, V. E., Cable, W. L., Walker, D. A., Kokelj, S. V., & Nicolsky, D. (2019). Climate Change Drives Widespread and Rapid Thermokarst Development in Very Cold Permafrost in the Canadian High Arctic. *Geophysical Research Letters*, *46*(12), 6681–6689. doi: 10.1029/2019GL082187

Forster, P., Storelvmo, T., K. Armour, W. Collins, J.-L. Dufresne, D. Frame, ... H. Zhang (2021). The Earth's Energy Budget, Climate Feedbacks, and Climate Sensitivity. In *Climate Change 2021: The Physical Science Basis. Contribution of Working Group I to the Sixth Assessment Report of the Intergovernmental Panel on Climate Change.* Cambridge University Press. (In Press.)

Fox-Kemper, B., Hewitt, H., Xiao, C., Adalgeirsdottir, G., Drijfhout, S., Edwards, T., ... Yu, Y. (2021). Ocean, Cryosphere and Sea Level Change. In *Climate Change 2021: The Physical Science Basis. Contribution of Working Group I to the Sixth Assessment Report of the Intergovernmental Panel on Climate Change.* Cambridge University Press. (In Press.)

Frederikse, T., Landerer, F., Caron, L., Adhikari, S., Parkes, D., Humphrey, V. W., ... Wu, Y.-H. (2020). The causes of sea-level rise since 1900. *Nature*, *584*(7821), 393–397. doi: 10.1038/s41586-020-2591-3

González-Rouco, J. F., Steinert, N. J., García-Bustamante, E., Hagemann, S., Vrese, P. d., Jungclaus, J. H., ... Navarro, J. (2021). Increasing the Depth of a Land Surface Model. Part I: Impacts on the Subsurface Thermal Regime and Energy Storage. *Journal of Hydrometeorology*, *22*(12), 3211–3230. doi: 10.1175/JHM-D-21-0024.1

Group, W. G. S. L. B. (2018). Global sea-level budget 1993–present. *Earth System Science Data*, *10*(3), 1551–1590. doi: 10.5194/essd-10-1551-2018

Hansen, J., Nazarenko, L., Ruedy, R., Sato, M., Willis, J., Genio, A. D., ... Tausnev, N. (2005). Earth's Energy Imbalance: Confirmation and Implications. *Science*, *308*(5727), 1431–1435. doi: 10.1126/science.1110252

Hermoso de Mendoza, I., Beltrami, H., MacDougall, A. H., & Mareschal, J.-C. (2020). Lower boundary conditions in land surface models – effects on the permafrost and the carbon pools: a case study with CLM4.5. *Geoscientific Model Development*, *13*(3), 1663–1683. doi: 10.5194/gmd-13-1663-2020

Hugelius, G., Strauss, J., Zubrzycki, S., Harden, J. W., Schuur, E. A. G., Ping, C.-L., ... Kuhry, P. (2014). Estimated stocks of circumpolar permafrost carbon with quantified uncertainty ranges and identified data gaps. *Biogeosciences*, *11*(23), 6573–6593. doi: 10.5194/bg-11-6573-2014

Jan, A., & Painter, S. L. (2020). Permafrost thermal conditions are sensitive to shifts in snow timing. *Environmental Research Letters*, *15*(8), 084026. doi: 10.1088/1748-9326/ab8ec4

Jorgenson, M. T., Shur, Y. L., & Pullman, E. R. (2006). Abrupt increase in permafrost degradation in Arctic Alaska. *Geophysical Research Letters*, *33*(2), L02503. doi: 10.1029/2005GL024960

Lacelle, D., Fisher, D. A., Verret, M., & Pollard, W. (2022). Improved prediction of the vertical distribution of ground ice in Arctic-Antarctic permafrost sediments. *Communications Earth & Environment*, *3*(1), 1–12. doi: 10.1038/s43247-022-00367-z

Langer, M., Nitzbon, J., Groenke, B., Assmann, L.-M., Schneider von Deimling, T., Stuenzi, S. M., & Westermann, S. (2022). The evolution of Arctic

permafrost over the last three centuries. *EGUsphere*. (Preprint) doi: 10.5194/egusphere-2022-473

Langer, M., Nitzbon, J., & Oehme, A. (2022a). *CryoGridLite: Model code for pan-Arctic simulations at 1° resolution from 1700 to 2020.* Zenodo. doi: 10.5281/zenodo.6619537

Langer, M., Nitzbon, J., & Oehme, A. (2022b). *CryoGridLite: Model input for pan-Arctic simulations at 1° resolution from 1700 to 2020.* Zenodo. doi: 10.5281/zenodo.6619212

Langer, M., Nitzbon, J., & Oehme, A. (2022c). *CryoGridLite: Model output of pan-Arctic simulations at 1° resolution from 1700 to 2020.* Zenodo. doi: 10.5281/zenodo.6619260

Lawrence, D. M., Slater, A. G., & Swenson, S. C. (2012). Simulation of Present-Day and Future Permafrost and Seasonally Frozen Ground Conditions in CCSM4. *Journal of Climate*, *25*(7), 2207–2225. doi: 10.1175/JCLI-D-11-00334.1

Lee, H., Swenson, S. C., Slater, A. G., & Lawrence, D. M. (2014). Effects of excess ground ice on projections of permafrost in a warming climate. *Environmental Research Letters*, *9*(12), 124006. doi: 10.1088/1748-9326/9/12/124006

Liljedahl, A. K., Boike, J., Daanen, R. P., Fedorov, A. N., Frost, G. V., Grosse, G., ... Zona, D. (2016). Pan-Arctic ice-wedge degradation in warming permafrost and its influence on tundra hydrology. *Nature Geoscience*, *9*(4), 312–318. doi: 10.1038/ngeo2674

Liu, L., & Larson, K. M. (2018). Decadal changes of surface elevation over permafrost area estimated using reflected GPS signals. *The Cryosphere*, *12*(2), 477–489. doi: 10.5194/tc-12-477-2018

Loeb, N. G., Johnson, G. C., Thorsen, T. J., Lyman, J. M., Rose, F. G., & Kato, S. (2021). Satellite and Ocean Data Reveal Marked Increase in Earth's Heating Rate. *Geophysical Research Letters*, e2021GL093047. doi: 10.1029/2021GL093047

Masson, V., Champeaux, J.-L., Chauvin, F., Meriguet, C., & Lacaze, R. (2003). A Global Database of Land Surface Parameters at 1-km Resolution in Meteorological and Climate Models. *Journal of Climate*, *16*(9), 1261–1282. doi: 10.1175/1520-0442(2003)16⟨1261:AGDOLS⟩2.0.CO;2

Mudryk, L. R., Derksen, C., Howell, S., Laliberté, F., Thackeray, C., Sospedra-Alfonso, R., ... Brown, R. (2018). Canadian snow and sea ice: historical trends and projections. *The Cryosphere*, *12*(4), 1157–1176. doi: 10.5194/tc-12-1157-2018

Nicolsky, D. J., & Romanovsky, V. E. (2018). Modeling Long-Term Permafrost Degradation. *Journal of Geophysical Research: Earth Surface*, *123*(8), 1756–1771. doi: 10.1029/2018JF004655

Nitzbon, J., Westermann, S., Langer, M., Martin, L. C. P., Strauss, J., Laboor, S., & Boike, J. (2020). Fast response of cold ice-rich permafrost in northeast Siberia to a warming climate. *Nature Communications*, *11*, 2201. doi: 10.1038/s41467-020-15725-8

Olefeldt, D., Goswami, S., Grosse, G., Hayes, D., Hugelius, G., Kuhry, P., ... Turetsky, M. R. (2016). Circumpolar distribution and carbon storage of thermokarst landscapes. *Nature Communications*, *7*, 13043. doi: 10.1038/ncomms13043

O'Neill, H. B., Wolfe, S. A., & Duchesne, C. (2019). New ground ice maps for Canada using a paleogeographic modelling approach. *The Cryosphere*, *13*(3), 753–773. doi: 10.5194/tc-13-753-2019

Pelletier, J. D., Broxton, P. D., Hazenberg, P., Zeng, X., Troch, P. A., Niu, G.-Y., ... Gochis, D. (2016). A gridded global data set of soil, intact regolith, and sedimentary deposit thicknesses for regional and global land surface modeling. *Journal of Advances in Modeling Earth Systems*, *8*(1), 41–65. doi: 10.1002/2015MS000526

Phipps, S. J., McGregor, H. V., Gergis, J., Gallant, A. J. E., Neukom, R., Steven-

son, S., ... Ommen, T. D. v. (2013). Paleoclimate Data–Model Comparison and the Role of Climate Forcings over the Past 1500 Years. *Journal of Climate*, *26*(18), 6915–6936. doi: 10.1175/JCLI-D-12-00108.1

Shur, Y. L., & Jorgenson, M. T. (2007). Patterns of permafrost formation and degradation in relation to climate and ecosystems. *Permafrost and Periglacial Processes*, *18*(1), 7–19. doi: 10.1002/ppp.582

Slater, A. G., Lawrence, D. M., & Koven, C. D. (2017). Process-level model evaluation: a snow and heat transfer metric. *The Cryosphere*, *11*(2), 989–996. doi: 10.5194/tc-11-989-2017

Slater, T., Lawrence, I. R., Otosaka, I. N., Shepherd, A., Gourmelen, N., Jakob, L., ... Nienow, P. (2021). Review article: Earth's ice imbalance. *The Cryosphere*, *15*(1), 233–246. doi: https://doi.org/10.5194/tc-15-233-2021

Smith, N. D., Burke, E. J., Schanke Aas, K., Althuizen, I. H. J., Boike, J., Christiansen, C. T., ... Chadburn, S. E. (2022). Explicitly modelling microtopography in permafrost landscapes in a land surface model (JULES vn5.4_microtopography). *Geoscientific Model Development*, *15*(9), 3603–3639. doi: 10.5194/gmd-15-3603-2022

Smith, S. L., O'Neill, H. B., Isaksen, K., Noetzli, J., & Romanovsky, V. E. (2022). The changing thermal state of permafrost. *Nature Reviews Earth & Environment*, *3*(1), 10–23. doi: 10.1038/s43017-021-00240-1

Steinert, N. J., González-Rouco, J. F., Melo Aguilar, C. A., García Pereira, F., García-Bustamante, E., de Vrese, P., ... Hagemann, S. (2021). Agreement of Analytical and Simulation-Based Estimates of the Required Land Depth in Climate Models. *Geophysical Research Letters*, *48*(20), e2021GL094273. doi: 10.1029/2021GL094273

Steinert, N. J., González-Rouco, J. F., Vrese, P. d., García-Bustamante, E., Hagemann, S., Melo-Aguilar, C., ... Lorenz, S. J. (2021). Increasing the Depth of a Land Surface Model. Part II: Temperature Sensitivity to Improved Subsurface Thermodynamics and Associated Permafrost Response. *Journal of Hydrometeorology*, *22*(12), 3231–3254. doi: 10.1175/JHM-D-21-0023.1

Stoy, P. C., Roh, J., & Bromley, G. T. (2022). It's the Heat and the Humidity: The Complementary Roles of Temperature and Specific Humidity to Recent Changes in the Energy Content of the Near-Surface Atmosphere. *Geophysical Research Letters*, *49*(4), e2021GL096628. doi: 10.1029/2021GL096628

Straneo, F., Adusumilli, S., Slater, D., Timmermans, M.-L., Marzeion, B., & Schweiger, A. (2020). *Data from: "Inventory of Earth's Ice Loss and Associated Energy Uptake from 1979 to 2017".* Zenodo. (10.5281/zenodo.4119129)

Strauss, J., Laboor, S., Schirrmeister, L., Fedorov, A. N., Fortier, D., Froese, D., ... Grosse, G. (2021). Circum-Arctic Map of the Yedoma Permafrost Domain. *Frontiers in Earth Science*, *9*.

Stuenzi, S. M., Boike, J., Gädeke, A., Herzschuh, U., Kruse, S., Pestryakova, L. A., ... Langer, M. (2021). Sensitivity of ecosystem-protected permafrost under changing boreal forest structures. *Environmental Research Letters*, *16*(8), 084045. doi: 10.1088/1748-9326/ac153d

Turetsky, M. R., Abbott, B. W., Jones, M. C., Anthony, K. W., Olefeldt, D., Schuur, E. A. G., ... McGuire, A. D. (2020). Carbon release through abrupt permafrost thaw. *Nature Geoscience*, *13*(2), 138–143. doi: 10.1038/s41561-019-0526-0

Turetsky, M. R., Abbott, B. W., Jones, M. C., Walter Anthony, K., Olefeldt, D., Schuur, E. A. G., ... Sannel, A. B. K. (2019). Permafrost collapse is accelerating carbon release. *Nature*, *569*, 32–34. doi: 10.1038/d41586-019-01313-4

von Schuckmann, K., Cheng, L., Palmer, M. D., Hansen, J., Tassone, C., Aich, V., ... Wijffels, S. E. (2020). Heat stored in the Earth system: where does the energy go? *Earth System Science Data*, *12*(3), 2013–2041. doi: https://doi.org/10.5194/essd-12-2013-2020

565 von Schuckmann, K., Palmer, M. D., Trenberth, K. E., Cazenave, A., Chambers,
566 D., Champollion, N., ... Wild, M. (2016). An imperative to monitor
567 Earth's energy imbalance. *Nature Climate Change*, *6*(2), 138–144. doi:
568 10.1038/nclimate2876
569 Westermann, S., Langer, M., Boike, J., Heikenfeld, M., Peter, M., Etzelmüller, B.,
570 & Krinner, G. (2016). Simulating the thermal regime and thaw processes of
571 ice-rich permafrost ground with the land-surface model CryoGrid 3. *Geosci.*
572 *Model Dev.*, *9*(2), 523–546. doi: 10.5194/gmd-9-523-2016
573 Wilkenskjeld, S., Miesner, F., Overduin, P. P., Puglini, M., & Brovkin, V. (2022).
574 Strong increase in thawing of subsea permafrost in the 22nd century caused
575 by anthropogenic climate change. *The Cryosphere*, *16*(3), 1057–1069. doi:
576 10.5194/tc-16-1057-2022
577 Zweigel, R. B., Westermann, S., Nitzbon, J., Langer, M., Boike, J., Etzelmüller,
578 B., & Schuler, T. V. (2021). Simulating Snow Redistribution and its Effect
579 on Ground Surface Temperature at a High-Arctic Site on Svalbard. *Jour-*
580 *nal of Geophysical Research: Earth Surface*, *126*(3), e2020JF005673. doi:
581 https://doi.org/10.1029/2020JF005673